Collective excitations and quantum incompressibility in electron-hole bilayers

S. De Palo,[1,2] P. E. Trevisanutto,[3,4] G. Senatore,[2] and G. Vignale [5]

[1]*CNR-IOM-DEMOCRITOS, Trieste, Italy*
[2]*Dipartimento di Fisica, Università di Trieste, strada Costiera 11, 34151 Trieste, Italy*
[3]*Centre for Advanced 2D Materials, National University of Singapore, 6 Science Drive 2, 117546 Singapore*
[4]*European Centre for Theoretical Studies in Nuclear Physics and Related Areas (ECT*-FBK) and Trento Institute for Fundamental Physics and Applications (TIFPA-INFN), Via Sommarive, 14, 38123 Povo TN, Trento, Italy*
[5]*Department of Physics and Astronomy, University of Missouri, Columbia, Missouri 65211, USA*

We apply quantum continuum mechanics to the calculation of the excitation spectrum of a coupled electron-hole bilayer. The theory expresses excitation energies in terms of ground-state intra- and interlayer pair correlation functions, which are available from quantum Monte Carlo calculations. The final formulas for the collective modes deduced from this approach coincide with the formulas obtained in the "quasilocalized particle approximation" by Kalman *et al.* [G. Kalman, V. Valtchinov, and K. I. Golden, Phys. Rev. Lett. **82**, 3124 (1999)], and likewise the theory predicts the existence of gapped excitations in the charged channel, with the gap arising from electron-hole correlation. An immediate consequence of the gap is that the static density-density response function of the charged channel vanishes as q^2 for wave vector $q \to 0$, rather than linearly in q, as commonly expected. In this sense, the system is *incompressible*. This feature, which has no analog in the classical electron-hole plasma, is consistent with the existence of an excitonic ground state and implies the existence of a discontinuity in the chemical potential of electrons and holes when the numbers of electrons and holes are equal. It should be experimentally observable by monitoring the densities of electrons and holes in response to potentials that attempt to change these densities in opposite directions.

I. INTRODUCTION

Two-dimensional electron-hole systems, in which electrons and holes reside in well-separated layers of a semiconductor heterostructure (see Fig. 1), have received much attention in recent years. Well separated means that tunneling between the layers is negligible. Voltages V_e and V_h applied to the electron (e) and hole (h) layers, respectively, can be used to control the carrier densities in each layer. The attractive interaction between electrons and holes creates a rich phase diagram in which BCS pairing at high density, exciton, and multiexciton formation at low density compete with the conventional Fermi liquid phase.

Quantum Monte Carlo (QMC) calculations of the ground-state wave function of this system have provided compelling evidence for the existence of non-Fermi liquid states with the formation of exciton and multiexciton complexes and the appearance of off-diagonal long-range order at low densities [1–6]. Experimental signatures of electron-hole pairing and superfluidity have been seen in counterflow experiments at high magnetic field [7,8] in multilayer structures of transition-metal dichalcogenides [9–12], and are also expected to emerge from Coulomb drag experiments [13] and in tunneling experiments [14]. In this paper, we will use the available information about the ground-state properties of the electron-hole bilayer to achieve something that is presently beyond the reach of QMC, namely, to predict the density fluctuation spectrum and the transverse current fluctuation spectrum.

We will focus on *symmetric* electron-hole systems, meaning that the densities and the effective masses of electrons and holes are identical and the elementary excitations can be classified as symmetric (electrons and holes moving in phase) and antisymmetric (electrons and holes moving out of phase).

The excitation spectrum is largely determined by the character of the ground state. For example, in the Fermi liquid phase, there are two types of excitations: single-particle excitations out of the Fermi sea and collective modes (plasmons), in which the electrons and the holes oscillate out of phase, with a dispersion $\propto \sqrt{q}$, where q is the wave vector. In principle, an acoustic plasmon mode could also exist, with electrons and holes oscillating in phase, at sufficiently large interlayer separation [15]. All these excitations are gapless. The transverse current excitation spectrum is also gapless.

The situation is quite different in electron-hole paired phases. A fundamental property of the paired ground state is its *rigidity* with respect to perturbations that tend to shift electron and hole densities in opposite directions. This can be understood as follows. Adding (or removing) equal numbers of electrons and holes in a small volume of the system can be viewed as increasing (or decreasing) the number of bound electron-hole pairs without breaking any bond. The sum of the addition and removal energies of a pair is $2\mu - 2\mu = 0$, where μ is the chemical potential and 2μ is the energy of a bound electron-hole pair: this is what we mean when we say that this mode of excitation is gapless. In contrast, adding
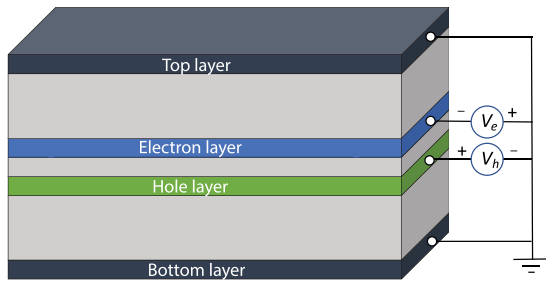
FIG. 1. Schematics of an electron-hole bilayer heterostructure. The densities of electrons and holes are controlled by changing the potentials of the electron and hole layers relative to the top and bottom layers (gates).

an electron while removing one hole changes the energy by $-2\mu + 2\epsilon_e$, where ϵ_e is the energy of a free (unbound) electron. Similarly, removing an electron while adding a hole changes the energy by $-2\mu + 2\epsilon_h$, where ϵ_h is the energy of a free (unbound) hole. The sum of the addition and removal energies is now $2(\epsilon_e + \epsilon_h - 2\mu)$, which is twice the binding energy of an electron-hole pair: hence, this mode of excitation is gapped.

To calculate the excitation spectra of electron-hole bilayers, we resort to quantum continuum mechanics (QCM—not to be confused with QMC) for quantum electronic systems. This theory was discussed in detail in Ref. [16]. It yields an exact equation of motion (Eq. (15) in Ref. [16]) for the current density in terms of a stress tensor field, which is, in principle, a functional of the current density itself. In the elastic approximation (see Ref. [16]), the equation of motion for the current is obtained by making an ansatz on the form of the solution of the time-dependent Schrödinger equation, namely, that the time-dependent wave function is obtained by applying a time-dependent deformation to the ground-state wave function. Equivalently, one can say that the wave function remains constant in an accelerated reference frame in which the density is constant and each infinitesimal volume element of the system remains at rest. Under these assumptions, the equation of motion for the current density can be expressed in terms of ground-state properties, such as the momentum occupation number and the pair distribution functions, which can be accurately computed by QMC. This approach is justifiable only for strongly interacting systems, whose dynamics is dominated by collective motions of relatively large groups of electrons (the volume elements of the fluid), while single-particle excitations are negligible or absent. For example, ^{4}He and electrons in the lowest Landau level [17] are well described by this method. Low-density electron liquids with strong Wigner crystal-like correlations between the positions of the electrons are expected to be well described too. Generally, the method works well for collective modes. The single-particle portion of the excitation spectrum, if present, is absorbed in the collective mode spectrum in such a way that certain spectral sum rules (*f*-sum rule, third moment sum rule) are satisfied.

In this paper, we apply QCM to the calculation of the excitation spectrum of an electron-hole bilayer. Remarkably, the final expressions for the collective mode frequencies coincide with the expressions that were obtained by Kalman *et al.* [18] by using what they called the "quasi-localized particle approximation" (QLCA). Thus, we can say that QCM offers a way to formalize the physical assumptions underlying the QLCA.

The most interesting result of the calculation is that the antisymmetric sector of the spectrum is gapped. Thus, in contrast to the Fermi liquid, where the antisymmetric mode (electrons and holes oscillating with opposite phases) is gapless with dispersion $q^{1/2}$, the QCM (like the QLCA) predicts a finite frequency $\omega(0)$—the gap—in the $q \to 0$ limit. The origin of the gap in QCM is easily traced to correlations between electrons and holes in opposite layers—the enhancement of the on-top electron-hole pair distribution function $g_{eh}(0)$ playing the key role. The gap is present for arbitrarily small values of the coupling parameter r_s, (although its value tends to zero very rapidly as $r_s \to 0$) and does not even require the presence of BCS-like pairing between electrons and holes. This suggests that the system is *never* a Fermi liquid—a conclusion that may be formally correct for electron-hole bilayers.

The gap in the antisymmetric density excitation spectrum of electron-electron bilayers was predicted in the classical (nondegenerate) regime [19] and was directly confirmed by classical molecular dynamic simulation. No such direct method is available for studying the dynamics of degenerate electron-hole systems. A semianalytic study [20,21] within the framework of QLCA (equivalent to the present approach) was carried out for degenerate *electron-electron* bilayers, but not for degenerate electron-hole bilayers.

There is an important difference between classical and quantum (degenerate) systems. In the classical system, the finite temperature effectively erases the most significant signature of the gap, namely, the rigidity (or incompressibility) of the system with respect to actions that attempt to change the densities of electrons and holes in opposite directions. The classical fluctuation-dissipation theorem [22] directly ties the density-density response function, which controls the response to external potentials, to the static structure factor. The latter vanishes linearly with q for the antisymmetric channel in the $q \to 0$ limit [23]. This indeed indicates a suppression of the density response for small q, but its origin is quite clear: It is the large electrostatic energy associated with adding electrons to one layer and removing holes from the other. In a realistic experimental setup, this charging energy will be neutralized by additional charges occurring on the gates, ultimately leaving us with a finite density response (that is to say, the so-called proper density-density response function [22], which does not vanish for $q \to 0$).

In contrast to this, the density-density response function of the gapped quantum system vanishes as q^2 for $q \to 0$. The vanishing density response is not caused by the charging energy, rather it reflects the energy cost of breaking bound electron-hole pairs as explained above. This kind of rigidity cannot be compensated by additional charges on the gates: it is present in the proper density-density response function itself.

Experimentally, rigidity would show up in measurements of the electron and hole densities as functions of applied gate voltages V_e and V_h. Starting from the symmetric situation $n_e = n_h$, the application of potentials V_e and V_h, which tend

to shift the electron and hole densities in opposite directions, will have no effect on the densities until the potentials exceed a threshold given by the gap [24].

This paper is organized as follows. In Sec. II and the Appendix, we review the elastic approximation of QCM and derive the formulas expressing the collective mode frequencies in terms of the pair distribution function and the kinetic energy of the ground state. We show that our formulas coincide with those of the QLCA. In Sec. III, we express the collective mode frequencies in terms of real-space integrals over the pair correlation functions and provide a simple formula, Eq. (18), expressing the gap in terms of the electron-hole interaction potential and the pair distribution function. In Sec. III A, we present and discuss the evaluation of the real-space integrals with pair correlation functions obtained from QMC, emphasizing the appearance of a gap in the antisymmetric density (longitudinal current) and transverse current channel. In Sec. III B, the same calculations are performed with pair correlation functions obtained, at much lower computational cost, from the solution of the BCS-like mean field theory. The pair correlation functions obtained in this manner are similar to the ones obtained in QMC, when the latter are available, and allow us to explore the behavior of the gap in a wider region of values of r_s and d. In Sec. IV, we discuss the antisymmetric density response function obtained from QCM with the antisymmetric density response function obtained from the BCS-like mean-field theory. Both response functions are found to vanish in the long-wavelength limit, implying incompressibility. The relation between the QCM gap and the BCS gap is clarified. In Sec. V we present a critical discussion of the elastic approximation vis-a-vis the so-called Bijl-Feynman approximation [25] which produces a spectrum consistent with the exact static structure factor but in violation of the third moment sum rule. Section VI contains a summary of our results for the excitation spectrum in the elastic approximation and our outlook on theoretical work going beyond the elastic approximation.

II. ELECTRON-HOLE BILAYER—MODEL AND ELASTIC APPROXIMATION FOR COLLECTIVE MODES

We consider a homogeneous symmetric electron-hole bilayer with Hamiltonian

$$H = \sum_{i,\alpha} \frac{p_{i\alpha}^2}{2m} + \frac{1}{2} \sum_{i \neq j} \sum_{\alpha} \phi_{\alpha\alpha}(|\mathbf{r}_{i,\alpha} - \mathbf{r}_{j,\alpha}|)$$
$$+ \sum_{i,j} \sum_{\alpha,\beta \neq \alpha} \phi_{\alpha\beta}(|\mathbf{r}_{i,\alpha} - \mathbf{r}_{j,\beta}|), \quad (1)$$

where the indices i and j run over the particles (either electrons or holes) of which there are equal numbers distributed with areal density $n = n_e = n_h$, and the indices α, β take values in the set (e, h) where e stands for electrons and h for holes. Thus $\mathbf{r}_{i,e}$ and $\mathbf{p}_{i,e}$ are the (two-dimensional) position and momentum of the ith electron and similarly for holes. The mass m is the same for electrons and holes. The electron-electron and hole-hole interactions are

$$\phi_{ee}(r) = \phi_{hh}(r) = \frac{e^2}{r}, \quad (2)$$

and

$$\phi_{eh}(r) = \phi_{he}(r) = -\frac{e^2}{\sqrt{r^2 + d^2}}, \quad (3)$$

where r is the distance between two electrons (holes) in the same layer, d is the distance between the layers, and $\sqrt{r^2 + d^2}$ is the distance between an electron and a hole in opposite layers. e is the absolute value of the electron charge. The strength of the Coulomb interaction is measured by the Wigner-Seitz parameter

$$r_s = \frac{1}{\sqrt{n\pi} a}, \quad (4)$$

where $a = \hbar^2/(me^2)$ is the Bohr radius.

We refer the reader to Ref. ([16]) for a detailed discussion of QCM and the elastic approximation. Here we only use the final result, which is an equation of motion for the displacement field $\mathbf{u}(\mathbf{r}, t)$, related to the current density by $\mathbf{j}(\mathbf{r}, t) = n(\mathbf{r})\dot{\mathbf{u}}(\mathbf{r}, t)$ where $n(\mathbf{r})$ is the ground-state density and $\dot{\mathbf{u}}(\mathbf{r}, t)$ is the time derivative of the displacement field, i.e., the velocity of the volume element. In the absence of external fields, this equation of motion has the form (see Eq. (46) in Ref. ([16]))

$$mn(\mathbf{r})\ddot{\mathbf{u}}(\mathbf{r}, t) = -\frac{\delta E_2[\mathbf{u}]}{\delta \mathbf{u}(\mathbf{r}, t)}, \quad (5)$$

where $E_2[\mathbf{u}]$ is a quadratic functional of the displacement field, obtained by expanding the energy (kinetic plus potential) to second order in the displacement field. (We note in passing that the system is assumed to have no net spin polarization: each volume element contains equal numbers of up- and down-spin particles, and they all follow the displacement field $\mathbf{u}$ regardless of spin orientation).

The expression on the right-hand side of Eq. (5) is a generalized force which, as shown in Ref. ([16]), can be expressed in terms of the one-particle density matrix and the pair distribution function of the ground state. Equation (5) defines a small-oscillation problem whose eigenfrequencies are the excitation energies. For an isotropic system, such as a uniform electron liquid, the longitudinal component of $\mathbf{u}$ yields the density excitation spectrum, and the transverse component yields the transverse current excitation spectrum. These approximate spectra consist of discrete excitation frequencies, at variance with the exact spectra, which are continuous. Yet, the spectral moments (first moment for the current fluctuation spectrum, first and third moments for the density fluctuation spectrum) can be shown to be exact, provided, of course, the input ground state information is exact.

To apply the QCM formalism to the electron-hole bilayer, we first generalize the formalism of Ref. ([16]) to a system with several components in dimension D. This is done in the Appendix. We then apply the formalism to a symmetric electron-hole system in two dimensions. This involves two displacement fields $\mathbf{u}_e(\mathbf{r}, t)$ and $\mathbf{u}_h(\mathbf{r}, t)$ for electrons and holes, respectively. They are related to the electron and hole current densities by $\mathbf{j}_\alpha(\mathbf{r}, t) = n\dot{\mathbf{u}}_\alpha(\mathbf{r}, t)$, where $\alpha = e$ or h, and n is the uniform density of electrons or holes. Equation (5) becomes a system of two coupled linear equations after the replacement $\mathbf{u} \to \mathbf{u}_\alpha$ and the recognition that the energy E_2 is a quadratic functional of both $\mathbf{u}_e$ and $\mathbf{u}_h$.

We take advantage of the translational invariance of the system (in the plane of the layers) by introducing the Fourier transform of the displacement fields, $\tilde{\mathbf{u}}_\alpha(\mathbf{q}, \omega)$, where $\mathbf{q}$ is the wave vector and ω is the frequency. The equation of motion takes the form

$$-mn\omega^2\tilde{\mathbf{u}}_\alpha = -\frac{\delta T_2[\tilde{\mathbf{u}}_\alpha]}{\delta\tilde{u}_\alpha} - \frac{\delta W_2[\tilde{\mathbf{u}}_e, \tilde{\mathbf{u}}_h]}{\delta\tilde{u}_\alpha}, \quad (6)$$

where T_2 and W_2 are, respectively, the kinetic and potential parts of the energy functional. The functional derivatives on the right-hand side of Eq. (6) are readily obtained from the appropriate two-component generalization of Eqs. (53) and (58) of Ref. ([16]). The formulas for the kinetic energy term are greatly simplified by dropping all the terms that contain the gradient of the ground-state density. The final expression is

$$\frac{\delta T_2[\tilde{\mathbf{u}}_\alpha]}{\delta\tilde{u}_\alpha} = nt(n)[2\mathbf{q}(\mathbf{q}\cdot\tilde{\mathbf{u}}_\alpha) + q^2\tilde{\mathbf{u}}_\alpha] + \frac{n\hbar^2 q^2}{4m}\mathbf{q}(\mathbf{q}\cdot\tilde{\mathbf{u}}_\alpha), \quad (7)$$

with $\alpha = e, h$, where $nt(n)$ is the kinetic energy per unit area of the interacting electron-hole system—a quantity well-known from QMC calculations. Notice that this kinetic force does not couple the displacement fields of different species.

The calculation of the potential energy term is more complex but the final result is quite simple:

$$\frac{\delta W_2[\tilde{\mathbf{u}}_e, \tilde{\mathbf{u}}_h]}{\delta\tilde{u}_\alpha} = \sum_{\beta,\nu}\{-[K_{\alpha\beta}(\mathbf{q}=\mathbf{0})]_{\mu\nu}\tilde{u}_{\alpha\nu}(\mathbf{q}) + [K_{\alpha\beta}(\mathbf{q})]_{\mu\nu}\tilde{u}_{\beta\nu}(\mathbf{q})\}, \quad (8)$$

where α and β take values e or h, and μ and ν are cartesian indices. The all-important kernel $[K_{\alpha\beta}(\mathbf{q})]_{\mu\nu}$ is calculated from the structure factors of the ground state, $S_{\alpha\beta}(q)$, as follows:

$$[K_{\alpha\beta}(\mathbf{q})]_{\mu\nu} = n\int\frac{d\mathbf{q}'}{(2\pi)^2}[S_{\alpha\beta}(|\mathbf{q}-\mathbf{q}'|) - \delta_{\alpha\beta}]\tilde{\phi}_{\alpha\beta}(q')q'_\mu q'_\nu + n^2 q_\mu q_\nu \tilde{\phi}_{\alpha\beta}(q), \quad (9)$$

where

$$S_{\alpha\beta}(\mathbf{q}) = \frac{1}{N}\sum_{n,n'}\langle e^{i\mathbf{q}\cdot(\mathbf{r}_{n,\alpha}-\mathbf{r}_{n'\beta})}\rangle - N\delta_{\mathbf{q},0}. \quad (10)$$

$\langle...\rangle$ denotes the ground state average and $\tilde{\phi}_{ee}(q) = \tilde{\phi}_{hh}(q) = \frac{2\pi e^2}{q}$, $\tilde{\phi}_{eh}(q) = \tilde{\phi}_{he}(q) = -\frac{2\pi e^2}{q}e^{-qd}$. Notice that the structure factors are expressible in terms of the Fourier transforms of the pair distribution functions for species α and β [22]; we will make use of this in the next section.

The symmetry of the problem ($S_{ee} = S_{hh}$, $S_{eh} = S_{he}$) allows us to decouple the equations of motion into symmetric/antisymmetric channels denoted by $+$ and $-$, respectively, defined as follows:

$$\tilde{u}_\pm(\mathbf{q}, \omega) = \tilde{u}_e(\mathbf{q}, \omega) \pm \tilde{u}_h(\mathbf{q}, \omega). \quad (11)$$

Furthermore, isotropy allows us to decouple the longitudinal channel ($\tilde{\mathbf{u}} \parallel \mathbf{q}$), denoted by L, from the transverse channel ($\tilde{\mathbf{u}} \perp \mathbf{q}$), denoted by T. Thus we arrive at the following explicit formulas for the frequencies of the longitudinal collective modes:

$$\omega_{L+}^2(\mathbf{q}) = \frac{2\pi ne^2 q}{m}(1 - e^{-qd}) + q^2\left[\frac{3t(n)}{m} + \frac{\hbar^2 q^2}{4m^2}\right] + \frac{1}{m}\int\frac{d\mathbf{q}'}{(2\pi)^2}[S_{ee}(|\mathbf{q}-\mathbf{q}'|) - S_{ee}(q')]\tilde{\phi}_{ee}(q')(\mathbf{q}'\cdot\hat{\mathbf{q}})^2$$
$$+ \frac{1}{m}\int\frac{d\mathbf{q}'}{(2\pi)^2}[S_{eh}(|\mathbf{q}-\mathbf{q}'|) - S_{eh}(q')]\tilde{\phi}_{eh}(q')(\mathbf{q}'\cdot\hat{\mathbf{q}})^2 \quad (12)$$

and

$$\omega_{L-}^2(\mathbf{q}) = \frac{2\pi ne^2 q}{m}(1 + e^{-qd}) + q^2\left[\frac{3t(n)}{m} + \frac{\hbar^2 q^2}{4m^2}\right] + \frac{1}{m}\int\frac{d\mathbf{q}'}{(2\pi)^2}[S_{ee}(|\mathbf{q}-\mathbf{q}'|) - S_{ee}(q')]\tilde{\phi}_{ee}(q')(\mathbf{q}'\cdot\hat{\mathbf{q}})^2$$
$$- \frac{1}{m}\int\frac{d\mathbf{q}'}{(2\pi)^2}[S_{eh}(|\mathbf{q}-\mathbf{q}'|) + S_{eh}(q')]\tilde{\phi}_{eh}(q')(\mathbf{q}'\cdot\hat{\mathbf{q}})^2, \quad (13)$$

where $\hat{\mathbf{q}}$ is the unit vector along $\mathbf{q}$. Similarly, for the transverse collective modes, we may set $\mathbf{q} = q\hat{x}$ to obtain

$$\omega_{T+}^2(\mathbf{q}) = q^2\frac{t(n)}{m} + \frac{1}{m}\int\frac{d\mathbf{q}'}{(2\pi)^2}[S_{ee}(|\mathbf{q}-\mathbf{q}'|) - S_{ee}(q')]\tilde{\phi}_{ee}(q')(q'_y)^2$$
$$+ \frac{1}{m}\int\frac{d\mathbf{q}'}{(2\pi)^2}[S_{eh}(|\mathbf{q}-\mathbf{q}'|) - S_{eh}(q')]\tilde{\phi}_{eh}(q')(q'_y)^2 \quad (14)$$

and

$$\omega_{T-}^2(\mathbf{q}) = q^2\frac{t(n)}{m} + \frac{1}{m}\int\frac{d\mathbf{q}'}{(2\pi)^2}[S_{ee}(|\mathbf{q}-\mathbf{q}'|) - S_{ee}(q')]\tilde{\phi}_{ee}(q')(q'_y)^2$$
$$- \frac{1}{m}\int\frac{d\mathbf{q}'}{(2\pi)^2}[S_{eh}(|\mathbf{q}-\mathbf{q}'|) + S_{eh}(q')]\tilde{\phi}_{eh}(q')(q'_y)^2. \quad (15)$$

The main qualitative features of the spectrum are immediately visible in these formulas. The symmetric channel spectrum is gapless because the expressions $[S_{ee}(|\mathbf{q}-\mathbf{q}'|) - S_{ee}(q')]$ and $[S_{eh}(|\mathbf{q}-\mathbf{q}'|) - S_{eh}(q')]$ in the integrals of Eqs. (12) and
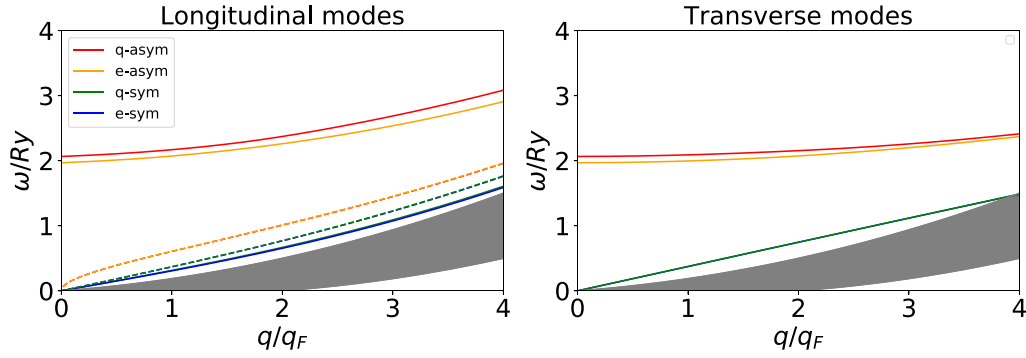
FIG. 2. Interlayer distance $d = 0.3$ a.u. Left panel: Longitudinal modes $\omega_{L-}(q)$, $\omega_{L+}(q)$. Right panel: Transverse modes $\omega_{T-}(q)$, $\omega_{T+}(q)$. The noninteracting single-particle spectrum is shown for reference as a shaded region. Solid lines: Dispersion of the antisymmetric mode in the quadriexcitonic (q) phase (red lines) and in the excitonic (e) phase (orange lines); dispersion of the symmetric mode in the quadriexcitonic phase (green lines) and in the excitonic phase (blue lines). Dashed lines with the same color coding present the dispersion of the modes calculated without the structure factor terms in Eqs. (12)–(15).

(14) vanish for $q \to 0$. In contrast, the antisymmetric channel spectrum, in which electrons and holes oscillate with opposite phases in the two layers, is gapped because the expression $[S_{eh}(|\mathbf{q} - \mathbf{q}'|) + S_{eh}(q')]$ in the integrand of Eqs. (13) and (15) *does not vanish* for $q \to 0$. The existence of electron-hole correlation, described by the structure factor $S_{eh}(q)$ and the associated pair distribution function $g_{eh}(r)$ is fully responsible for the emergence of the gap.

III. REAL-SPACE IMPLEMENTATION

We now calculate the frequency of the collective modes, Eqs. (12)–(15), using real-space pair-correlation functions $g_{eh}(r)$ and $g_{ee}(r)$ [6]. For example, the integral

$$I_{\alpha\beta}^{\pm}(q) = \int \frac{d\mathbf{q}'}{(2\pi)^2} [S_{\alpha\beta}(|\mathbf{q} - \mathbf{q}'|) \pm S_{\alpha\beta}(q')] \tilde{\phi}_{\alpha\beta}(q')(\mathbf{q}' \cdot \hat{\mathbf{q}})^2 \tag{16}$$

can be rewritten as

$$I_{\alpha\beta}^{\pm}(q) = 2\pi n \int_0^{\infty} dr\, r h_{\alpha\beta}(r) \left\{ \frac{1}{2} [J_0(qr) - J_2(qr) \pm 1] \right.$$
$$\times \left[\frac{\phi_{\alpha\beta}'(r)}{r} - \phi_{\alpha\beta}''(r) \right] - [J_0(qr) \pm 1] \frac{\phi_{\alpha\beta}'(r)}{r} \Bigg\}, \tag{17}$$

where $h_{\alpha\beta}(r) = g_{\alpha\beta}(r) - 1$ and $J_n(qr)$ are Bessel functions of order n.

Notice that the $\pm$ signs in Eq. (17) make the all-important difference between the gapless spectrum in the symmetric channel and the gapped one in the antisymmetric channel. The square of the gap is given by

$$\omega^2(0) = -\frac{1}{m} I_{e,h}^+(0) = \frac{n}{m} \int d\mathbf{r}\, h_{e,h}(r) \nabla^2 \phi_{e,h}(r), \tag{18}$$

which (in Rydberg^2) is given by the simple formula

$$\omega^2(0) = \frac{8}{r_s^2} \int_0^{\infty} dr\, h_{eh}(r) r \frac{2d^2 - r^2}{(r^2 + d^2)^{5/2}}, \tag{19}$$

where r, d are in atomic units. This has the same value for the longitudinal and the transverse mode.

A. Calculation with QMC pair correlation functions

In Figs. 2–4, we plot the dispersion of the symmetric and antisymmetric modes, longitudinal (left panels) and transverse (right panels) obtained by evaluating the real-space integrals Eq. (17) with QMC pair correlation functions. Results are presented for $r_s = 4$ and four different values of the interlayer
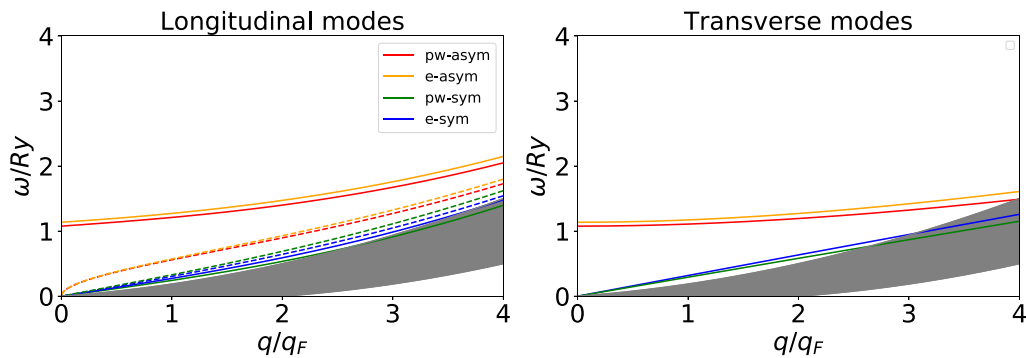

FIG. 3. Interlayer distance $d = 0.5$ a.u. Left panel: Longitudinal modes $\omega_{L-}(q)$, $\omega_{L+}(q)$. Right panel: Transverse modes $\omega_{T-}(q)$, $\omega_{T+}(q)$. The noninteracting single-particle spectrum is shown for reference as a shaded region. Solid lines: Dispersion of the antisymmetric mode in the excitonic (e) phase (orange lines) and in the plasma (pw) phase (red lines); dispersion of the symmetric mode in the excitonic phase (blue lines) and in the plasma phase (green lines). Dashed lines with the same color coding present the dispersion of the modes calculated without the structure factor terms in Eqs. (12)–(15).
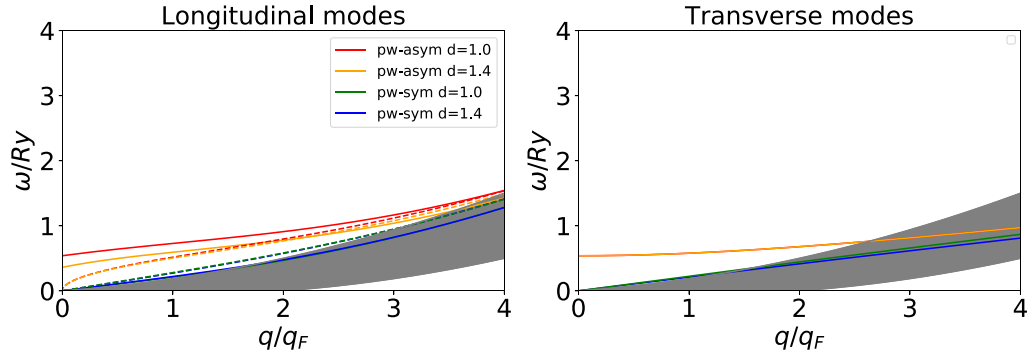
FIG. 4. Interlayer distances $d = 1.0$ a.u. and $d = 1.4$ a.u, plasma phase (pw). Left panel: Longitudinal modes $\omega_{L-}(q)$, $\omega_{L+}(q)$. Right panel: Transverse modes $\omega_{T-}(q)$, $\omega_{T+}(q)$. The noninteracting single-particle spectrum is shown for reference as a shaded region. Solid lines: Dispersion of the antisymmetric mode for interlayer distance $d = 1.0$ a.u. (red lines) and $d = 1.4$ a.u. (orange lines); dispersion of the symmetric mode for interlayer distance $d = 1.0$ a.u. (green lines) and $d = 1.4$ a.u. (blue lines). Dashed lines with the same color coding present the dispersion of the modes calculated without the structure factor terms in Eqs. (12)–(15).

distance $d = 0.3$ a.u., $d = 0.5$ a.u., $d = 1.0$ a.u., $d = 1.4$ a.u. Because the QMC calculations assumed two equivalent valleys and two equivalent spin orientations in each layer, the Fermi wave vector q_F, which we use as the wave vector unit in these figures, is related to the density by $q_F = \sqrt{\pi n}$.

It is evident that the asymmetric modes display a finite gap for $q \to 0$. Such a gap is largest at the smallest distance considered ($d = 0.3$) and decreases for larger distances.

B. Calculation with BCS pair correlation functions

The QMC calculation of the pair correlation functions is time-consuming and the results are available only for a few values of r_s and d. We achieve much greater flexibility by resorting to the BCS-like mean-field theory of Refs. [26,27]. The crucial pair correlation function $h_{eh}(r)$ in this approach is

given by

$$h_{eh}^{\text{BCS}}(r) = \left| \frac{1}{n} \int_0^\infty \frac{dk\,k}{2\pi} \frac{\Delta(k)}{E(k)} J_0(kr) \right|^2, \qquad (20)$$

where the BCS gap function $\Delta(k)$ and the BCS quasiparticle energy $E(k) = \sqrt{\xi(k)^2 + \Delta(k)^2}$ are obtained from the self-consistent solution of the mean-field equations [26,27], where the k dependence of the gap, as well as the in-plane interaction, are taken into account.

$h_{eh}(r)$ calculated in this manner is in quite good agreement with the QMC result in the cases in which the latter is available. More importantly, using $h_{eh}^{\text{BCS}}(r)$ in Eq. (19) we can calculate $\omega(0)$ for a broad range of values of r_s and d. The results of the calculation are plotted in Fig. 5. A remarkable feature of these results is that in the low-density limit, ($r_s \to \infty$) $\omega(0)$ approaches a finite limit, independent of r_s. This is physically expected since in this limit the system reduces to a collection of well-separated bound electron-hole pairs and the pair correlation function becomes

$$h_{eh}(r) = n^{-1} |\psi_{eh}(r)|^2, \qquad (21)$$

where $\psi_{eh}(r)$ is the wave function of the bound state. In the opposite limit of high density ($r_s \to 0$) and finite d, the BCS gap goes to zero and so does $\omega(0)$.

Another interesting feature of the result is the logarithmic divergence of $\omega(0)$ in the limit of vanishing interlayer separation ($d \to 0$). Mathematically, this arises from the two-dimensional integration of the Coulomb interaction, which diverges at $r = 0$. This logarithmic divergence is likely to be an artifact of the elastic approximation. This will become more evident in the next section, where we relate $\omega(0)$ to the long-wavelength behavior of the antisymmetric density response function and hence to the incompressibility.

FIG. 5. Plot of $\omega(0)$ vs d for different values of r_s. $\omega(0)$ is calculated from Eq. (19) and the pair correlation function is obtained from the self-consistent solution of the BCS mean-field theory, according to Eq. (20), as explained in the text.

IV. ANTISYMMETRIC DENSITY RESPONSE AND INCOMPRESSIBILITY

In this section, we focus on the longitudinal spectrum in the antisymmetric channel. Unless otherwise indicated ω_q will be a shorthand for $\omega_{L-}(q)$. Similarly, $\chi(q, \omega)$ will be shorthand for $\chi_{L-}(q, \omega) \equiv \chi_{ee}(q, \omega) - \chi_{eh}(q, \omega)$ and $S(q)$ will be shorthand for $S_{L-}(q) \equiv S_{ee}(q) - S_{eh}(q)$.
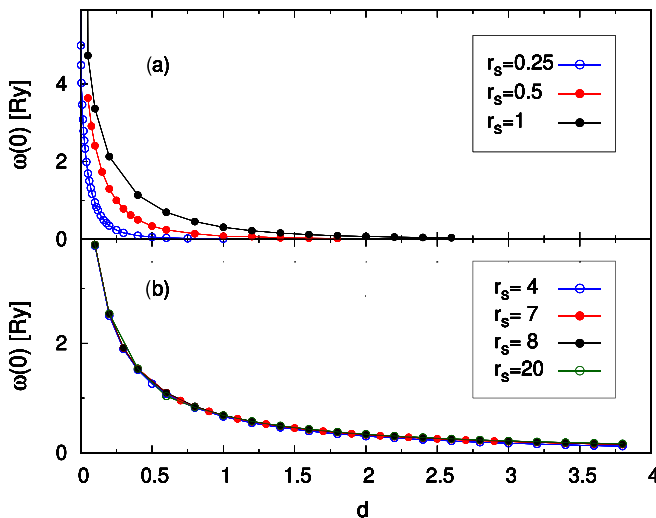
It is well-known [16] that the elastic approximation for a one-component system satisfies the so-called third moment sum rule for the density fluctuation spectrum. In our two-component system, the sum rule reads

$$-\frac{2}{\pi}\int_0^\infty d\omega \omega^3 \Im m \chi(q,\omega) = M(q)q^2, \qquad (22)$$

where $M(q)$ (standing for $M_{L-}(q)$, as explained above) is expressed in terms of the exact kinetic energy and structure factors as [22,28]

$$M(q) = \frac{n}{m}\left\{\frac{2\pi ne^2 q}{m}(1+e^{-qd}) + q^2\left[\frac{3t(n)}{m} + \frac{\hbar^2 q^2}{4m^2}\right]\right.$$
$$+ \frac{1}{m}\int \frac{d\mathbf{q}'}{(2\pi)^2}[S_{ee}(|\mathbf{q}-\mathbf{q}'|) - S_{ee}(q')]\tilde{\phi}_{ee}(q')(\mathbf{q}'\cdot\hat{\mathbf{q}})^2$$
$$- \frac{1}{m}\int \frac{d\mathbf{q}'}{(2\pi)^2}[S_{eh}(|\mathbf{q}-\mathbf{q}'|) + S_{eh}(q')]$$
$$\left.\times \tilde{\phi}_{eh}(q')(\mathbf{q}'\cdot\hat{\mathbf{q}})^2\right\}. \qquad (23)$$

On the other hand, a simple calculation starting from the equation of motion for the antisymmetric longitudinal mode, in the presence of external potentials acting on particles and identifying $-in\mathbf{q}\cdot\mathbf{u}_\gamma$ with the density change δn_γ, allows the calculation of the response function in the elastic approximation of QCM as

$$-\frac{1}{\pi}\Im m \chi_{QCM}(q,\omega) = \frac{nq^2}{2m\omega_q}[\delta(\omega-\omega_q)-\delta(\omega+\omega_q)]. \qquad (24)$$

It is immediately verified that the QCM response in the elastic approximation satisfies both the f-sum rule [22]

$$-\frac{2}{\pi}\int_0^\infty d\omega \omega \Im m \chi_{QCM}(q,\omega) = \frac{nq^2}{m}, \qquad (25)$$

and the third moment sum rule

$$-\frac{2}{\pi}\int_0^\infty d\omega \omega^3 \Im m \chi_{QCM}(q,\omega) = \frac{nq^2}{m}\omega_q^2 = M(q)q^2, \quad (26)$$

as from Eqs. (13) and (22):

$$\omega_q = \sqrt{\frac{mM(q)}{n}}. \qquad (27)$$

Notice that $M(q)$ tends to a finite limit for $q \to 0$, as discussed above. This is a unique feature of the antisymmetric density channel: in the symmetric density channel, the corresponding quantity $M_{L+}(q)$ is known to vanish as q^2 for $q \to 0$.

These reassuring results help us understand why our formulas for the collective mode frequencies coincide with those of Kalman *et al.*, obtained from the QLCA. Both theories collapse the spectrum onto a single collective mode which satisfies the third- and first-moment sum rules: these constraints are strong enough to uniquely determine the frequencies.

Let us now consider the static density response, which is given by the dispersion relation

$$\chi(q,0) = \frac{2}{\pi}\int_0^\infty d\omega \frac{\Im m \chi(q,\omega)}{\omega} \qquad (28)$$

(notice that this can be considered a negative-first-moment sum rule). Use of Eq. (24) yields the static response in QCM:

$$\chi_{QCM}(q,0) = -\frac{nq^2}{m\omega_q^2}. \qquad (29)$$

The existence of a finite gap ($\omega_q \to \omega_0 \equiv \omega(0) > 0$) for $q \to 0$ immediately implies that $\chi_{QCM}(q,0)$ vanishes as q^2. We emphasize that the vanishing of $\chi_{QCM}(q,0)$ is stronger than what would be expected from purely electrostatic considerations, e.g., from the random phase approximation, if the compressibility remained finite. Indeed, in the $q \to 0$ limit, the static response is related to the compressibility K_- (in the antisymmetric density channel) by the relation

$$\chi(q,0) \overset{q\to 0}{\to} -\frac{1}{v_{q-} + \frac{1}{n^2 K_-}}, \qquad (30)$$

where $v_{q-} = \frac{2\pi e^2}{q}(1+e^{-qd})$ and

$$\frac{1}{n^2 K_-} = 2\frac{\partial^2 \epsilon(n,\delta n_-)}{(\partial \delta n_-)^2}\bigg|_{n_e=n_h=n} \qquad (31)$$

is twice the second derivative of the energy density with respect to the imbalance density $\delta n_- = n_e - n_h$ evaluated at the charge neutrality point. (Notice that ϵ in this formula is the energy of a charge-neutral system, that is to say, we assume that the charge imbalance associated with δn_- is neutralized by compensating background charges at zero energy cost.) Now if K_- were finite, then $\chi(q,0)$ would vanish as q, due to the divergence of v_{q-} in the denominator of Eq. (30). But we have seen that $\chi(q,0)$ vanishes as q^2: this can be reconciled only if K_- is zero. More pointedly, we could introduce a q-dependent compressibility $K_-(q)$, whose inverse is the second derivative of the energy with respect to the amplitude of a density fluctuation of wave vector q. This q-dependent compressibility, replacing K_- in Eq. (30) would vanish as q^2 in the $q \to 0$ limit.

The QCM prediction of the existence of a gap $\omega(0)$ in the uniform (non-BCS) plasma phase of the electron-hole liquid is quite surprising: In this phase, one would expect to find a gapless plasmon, dispersing as $q^{1/2}$. On the other hand, the existence of a gap is completely expected in the paired BCS or excitonic phase because the formation of bound electron-hole pairs prevents long-range charge separation. In Sec. III, we used the BCS model as a practical tool to calculate pair correlation functions to be fed into the QCM machinery. Now we proceed to a more direct comparison between the physical predictions of QCM and BCS-like mean field theory. In particular, we compare the antisymmetric density response obtained in QCM [see Eq. (29)] with the same response calculated within the BCS-like mean field theory.

We start from the observation that in the BCS-like theory [26,27], the density response function in the antisymmetric channel is given by

$$\chi(q,0) = -q^2\frac{g_c}{32\pi}\int_0^\infty dk\, k\frac{[\xi(k)\Delta'(k)-\xi'(k)\Delta(k)]^2}{[\Delta(k)^2+\xi(k)^2]^{5/2}}, \qquad (32)$$

where g_c is the number of fermionic components per layer (here $g_c = 4$) and the quantities $\xi(k)$ and $\Delta(k)$ here are per particle, i.e., half of those in Ref. [26], which are per exciton
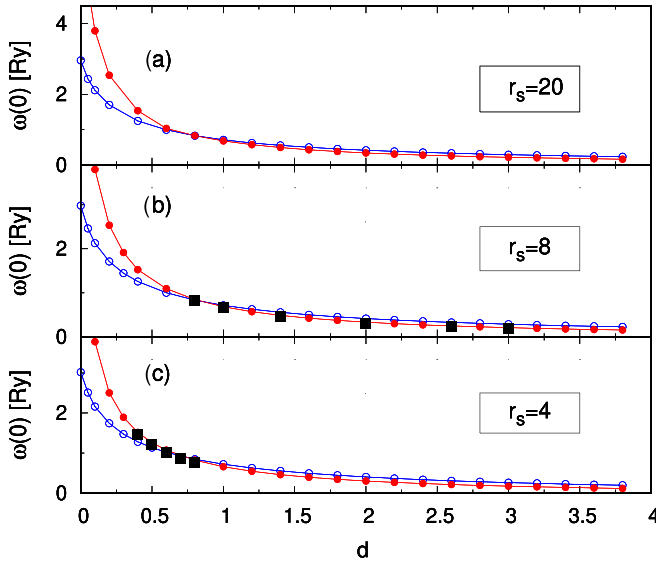
FIG. 6. Plot of $\omega(0)$ as a function of distance d for $r_s = 20, 8$ and 4, respectively, in (a)–(c). The solid red dots are calculated from Eq. (19) using the pair correlation function obtained from the self-consistent solution of the BCS mean field theory, according to Eq. (20). The solid black squares are obtained using the pair correlation functions from QMC simulations [6]. The open blue dots are the values of $\omega(0)$ obtained from the direct comparison of Eqs. (32) and (29).

FIG. 7. Plot of $\omega(0)$ as a function of r_s for various values of the distance d. Solid red and blue lines are, respectively, for $\omega_{\rm QCM}(0)$ and $\omega_\chi(0)$. The solid orange line is for $\omega_{\rm BF}(0)$, which is the $q \to 0$ limit of the Bijl-Feynman frequency, Eq. (36), calculated with the BCS structure factor of Eq. (37), as explained in Sec. V. The dashed black line is $\omega_{\rm QCM}(0)$ for a system made of isolated excitons, with the $h_{eh}(r)$ from Eq. (21). The solid dark-green line is -2μ. (a)–(c) show data for $d = 1, 0.5$ and 0.05, respectively.

(electron-hole pair). The prime denotes the derivative of a function with respect to its own argument.

The static response of the excitonic state assumes a particularly transparent form in the low-density limit, whereby to leading order in the density n it becomes

$$\chi(q, 0) = -q^2 \frac{g_c n}{32\pi |\mu|} \int_0^\infty dk k \frac{[\tilde{\psi}'_{eh}(k)]^2}{1 + (\xi k)^2}. \quad (33)$$

In the above formulas, $|\mu|$ and $\tilde{\psi}_{eh}(k)$ are, respectively, half the binding energy of the isolated exciton and the Fourier transform of its normalized wave function; also, $\xi^2 = \hbar^2/(2m|\mu|)$. For zero interlayer distance, the wave function of the isolated exciton ($\mu = -\hbar^2/(2ma_B^2)$) is known in closed form, $\tilde{\psi}_{eh}(k) = 2\sqrt{2\pi} a_B/[1 + (ka_B)^2]^{3/2}$. The integral in Eq. (33) can be readily performed and by comparison with Eq. (29), one gets $\hbar\omega(0) = 2\sqrt{(20/9)}Ry$.

In the opposite limit of high density (small r_s), there is no known simplification of Eq. (32). However, we have found that even at $d = 0$ the numerical solution with a finite gap function to the BCS equations [26] is lost for $r_s \lesssim 0.04$, implying that the system turns to the normal state. Thus, at least at the RPA level the static response becomes linear in q, implying the disappearance of the gap, i.e., $\omega(0) = 0$.

In Figs. 6 and 7, we show the values of $\omega(0)$ obtained from the direct comparison of Eqs. (32) and (29) (blue curves) versus the values of $\omega(0)$ obtained from Eq. (19) together with the pair correlation function given by Eq. (20) (red curves). In the following, the gap obtained from the BCS response will be referred to as $\omega_\chi(0)$ and the one obtained from the
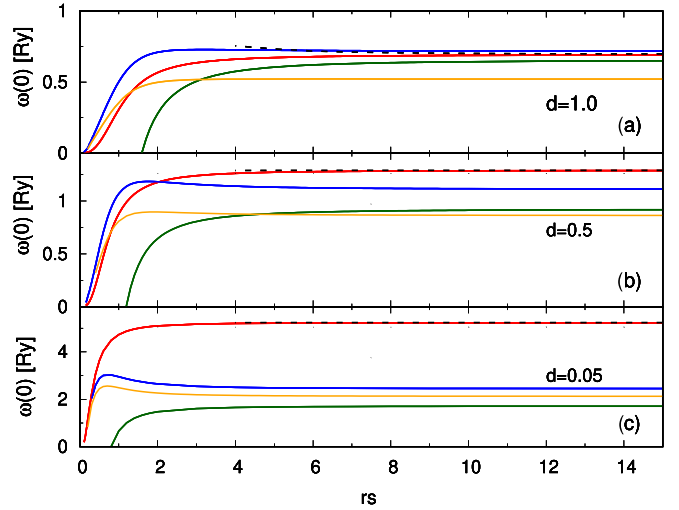
QCM will be referred to as $\omega_{\rm QCM}(0)$. The agreement between the two sets of values is generally quite good, particularly for large r_s and d. However, for small d, the QCM gap (red curve) is much too large in comparison with the one from the BCS response: this reflects the existence of an artificial logarithmic divergence of $\omega_{\rm QCM}(0)$ for $d \to 0$, as was pointed out at the end of Sec. III. Interestingly, there are also regions of parameter space (small r_s, large d) in which the QCM gap is *smaller* than the one from the BCS response, however, the difference between the two estimations of the gap is quite small in these regions.

Figure 7 shows the existence of a tight connection between $\omega(0)$ and the exciton binding energy in the low density limit and for large d. This is illustrated by the solid green line which shows -2μ vs r_s, with μ the chemical potential calculated within BCS theory. As discussed in the introduction, the binding energy of an electron-hole pair is given by $\epsilon_e + \epsilon_h - 2\mu$ where ϵ_e, ϵ_h are the energies of free (unbound) electrons and holes, respectively. In the low-density limit ϵ_e and ϵ_h are the energies of electrons and holes at the bottom of the respective bands, which we take to be at zero energy. Thus -2μ is the binding energy of the pair in this limit: indeed, we see that it approaches $\omega(0)$ for large r_s and d. This is important because the exciton binding energy is a quantity that can be determined experimentally by measuring the variations of the densities of electrons and holes as we apply potentials V_e and V_h which push them in opposite directions (see Fig. 1). Incompressibility means that the system will resist the push and remain balanced ($n_e = n_h$) in a range of potentials of order ϵ_b due to the rigidity associated with electron-hole pairing, as explained in the introduction. See Ref. [24] for details.

V. DISCUSSION

The quantum continuum mechanics is a formally exact theory of quantum dynamics[16], but the elastic approximation, on which the present paper is based, makes the questionable assumption that the time-dependent wave function is, at every instant of time t, obtained by applying a deformation with displacement field $\mathbf{u}(\mathbf{r}, t)$ to the ground-state wave function. Under this assumption, the excitation spectrum is reduced to a set of sharp normal modes, which describe collective density and current oscillations. This collective description of the dynamics is expected to be qualitatively correct in strongly correlated systems, where the single-particle degrees of freedom are effectively suppressed as the individual particles are enslaved to collective modes. In this section, we briefly discuss some issues that arise in connection with the approximate character of the theory.

One drawback of the elastic approximation becomes evident when we consider the fluctuation-dissipation theorem, which actually takes the form of a zeroth-moment sum rule or S-sum rule as follows:

$$-\frac{\hbar}{\pi n}\int_0^\infty d\omega\, \Im m\, \chi(q, \omega) = S(q). \tag{34}$$

As in the previous section, $\Im m\, \chi(q, \omega)$ and $S(q)$ denote the spectral density and the structure factor in the *antisymmetric* density-fluctuation channel. In general, the QCM formula for the spectral function in the elastic approximation fails to satisfy this sum rule, even as it satisfies the third-moment sum rule exactly. For example, in the high-density degenerate plasma phase, where the random phase approximation is valid, we know that the exact $S(q)$ must tend to zero as $q^{3/2}$ for $q \to 0$. But even in that case, the elastic approximation predicts a spectral gap, and hence $S(q) \propto q^2$ for $q \to 0$, as we can easily verify from our expression Eq. (24).

An approximation that satisfies the S-sum rule (but violates the third-moment sum rule) is known as Bijl-Feynman (BF) approximation [25] and yields the following formula for the spectral function:

$$-\frac{1}{\pi}\Im m\, \chi_{\mathrm{BF}}(q, \omega)$$
$$= \frac{n}{\hbar}S(q)[\delta(\omega - \omega_{\mathrm{BF}}(q)) - \delta(\omega + \omega_{\mathrm{BF}}(q)), \tag{35}$$

with

$$\omega_{\mathrm{BF}}(q) \equiv \frac{\hbar q^2}{2mS(q)}, \tag{36}$$

to satisfy the f-sum rule. In the uniform plasma phase (without BCS pairing), $S(q)$ vanishes as $q^{3/2}$ for $q \to 0$—a property that reflects the electrostatic energy of long-range charge density fluctuations. Thus, the BF dispersion of the uniform plasma phase is necessarily gapless and goes as $q^{1/2}$ for $q \to 0$ as expected for the classical plasmon in two dimensions. Similarly, if we consider the static density-density response function $\chi(q, 0)$, obtained from Eq. (28), we see that the BF approximation predicts $\chi_{\mathrm{BF}}(q, 0) \sim q \sim 1/v_{q-}$. Comparison with Eq. (30) shows that the antisymmetric compressibility K_- may vanish at most as q^α with $0 \leqslant \alpha < 1$.

Compared to the BF approximation, the elastic approximation of QCM has two major advantages. First, it gives a richer spectrum of collective modes, including both longitudinal and transverse excitations. Second, it expresses the frequencies of collective modes in terms of real space integrals, which are dominated by the short-range part of the pair correlation functions [see, for example, Eqs. (18) and (19)]. This is a crucial advantage in practical applications, since the short-range behavior of the pair correlation functions is more easily accessible in QMC simulations and less sensitive to finite-size effects than the small-q behavior of the structure factor, which appears in the BF expression Eq. (36).

On the other hand, because of its collective character the elastic approximation (equivalent to QLCA) predicts a spectral gap at all densities, even in the limit of quantum degenerate plasma where no gap is expected as discussed above.

This problem is not too severe in the present study because the electron-hole system is expected to spontaneously form Cooper pairs—thus abandoning the normal degenerate plasma phase—even at very high density. The antisymmetric structure factor of the paired phase vanishes as q^2, as one can easily verify from BCS theory [26,27], yielding

$$S(q) = -q^2 \frac{1}{8\pi n}\int_0^\infty dk\, k\, \frac{[\xi(k)\Delta'(k) - \xi'(k)\Delta(k)]^2}{[\Delta(k)^2 + \xi(k)^2]^2}, \tag{37}$$

and this gives, via Eq. (36), a gapped dispersion $\omega_{\mathrm{BF}}(0) > 0$, which is compared with $\omega_{\mathrm{QCM}}(0)$ and $\omega_\chi(0)$ in Fig. 7. The only issue here is that the elastic approximation overestimates the gap, possibly by a large factor, as discussed in the previous section. Otherwise, our results are qualitatively correct.

The prediction of a spectral gap is more problematic in systems with purely repulsive interactions—for example, electron-electron bilayers. In such systems, no Cooper pairs are expected to form in the degenerate high-density limit, and therefore the system should remain gapless. This contradicts the prediction of the QCM in the elastic approximation. Nevertheless, it is quite possible that a gap, qualitatively similar to what QCM predicts, will appear when the density is lowered below a certain critical value, at which the system enters a strongly correlated phase. This scenario is strongly suggested by the classical simulations of Ref. [19], which show the existence of a gapped out-of-phase mode in the strongly correlated classical electron-electron system. We may expect that the gap of the classical collective mode will manifest as a gap in the excitation spectrum of the corresponding quantum system. If this expectation is correct, then a quantum phase transition must occur at some critical density, separating the gapless phase on the high-density side from the gapful phase on the low-density side. However, we find no evidence of such a transition in the present theory.

One way to improve our treatment would be to modify the elastic approximation in such a way that it satisfies *both* the third-moment sum rule and the S-sum rule. How to do this in a controlled manner remains an interesting question for further study.

VI. SUMMARY AND OUTLOOK

Let us recapitulate our main findings.

(1) The elastic approximation of QCM, applied to electron-hole bilayers, is equivalent to QLCA: this provides insight into

the physical significance as well as the limits of validity of that approximation.

(2) Like QLCA, the theory predicts a gapped collective mode in the antisymmetric channel (i.e., when the carriers in the two layers oscillate with opposite phases). The frequency of this mode remains finite in the $q \to 0$ limit and this finite value, denoted by $\omega(0)$, is the gap.

(3) The gap is found to exist at all densities, even though it becomes vanishingly small in the high-density limit as $h_{eh}(r)$ tends to 0 [see Eq. (19)]. For the electron-hole bilayer, this prediction makes perfect physical sense. Indeed, the BCS mean-field theory applied to this system predicts the formation of Cooper pairs of electrons and holes with exponentially small binding energy at high density, evolving to exciton pairs at low density. This is at variance with electron-electron bilayers, where the ordinary Fermi liquid phase is expected to be stable at high density.

(4) A direct consequence of the gap, which has no equivalent in classical bilayers, is the incompressibility of the ground state, by which we mean the vanishing of the static density response function $\chi_-(q)$ as q^2 for $q \to 0$. The suppression of $\chi_-(q)$ at small q is much stronger than the suppression expected from the RPA for a compressible electron gas ($\chi_{RPA}(q) \sim q$), and reflects the finite binding energy of electron-hole pairs.

(5) The values of $\omega(0)$ calculated from the electron-hole pair distribution function of the QMC are in good agreement with those obtained from the pair distribution function of the BCS-like mean field theory. They are also in good agreement with the values obtained by comparing the BCS density response function with the density response function obtained in QCM. However, in this case, the good agreement breaks down in the limit of zero interlayer separation because QCM predicts a logarithmic divergence of $\omega(0)$ for $d \to 0$, which would make the density response function vanishes faster than q^2 for $q \to 0$.

(6) Our findings show that the QCM gap $\omega(0)$ calculated from a reliable set of pair distribution functions can be meaningfully related to the binding energy of bound states (excitons) for sufficiently large d and r_s.

(7) Incompressibility implies that the chemical potential of an electron has a discontinuous jump as a function of electron density n_e, when n_e crosses the hole density n_h. The jump in chemical potential equals the binding energy and can be measured experimentally by monitoring the electron and hole densities or the capacitance as functions of the voltages applied to the gates, as discussed in Ref. [12,24].

One drawback of our approach (QCM or QLCA) is that it predicts a gap in the out-of-phase mode at all densities *even in systems with only repulsive interactions* such as, for example, the *electron-electron* bilayer. This is in conflict with the expectation that such systems should be ordinary Fermi liquids at high density. Physically, we do not expect the elastic approximation to work well at high density because the excitation spectrum (in the antisymmetric channel) becomes increasingly single-particle-like. On the other hand, the low-density/strongly correlated limit should be described correctly if we assume that the electrons in the two layers freeze into two interlocking Wigner-crystal structures. In the case of electron-hole bilayers, this correlated regime may set in even at high density, due to the occurrence of the Cooper instability. It has not been possible so far to formulate a criterion to determine at what density, if any, the gap predicted by the present theory would cease to be reliable. We speculate that, with such criterion in hand, one could identify a quantum phase transition between a gapless phase at high density and a gapful one at low density.

APPENDIX: ELASTIC APPROXIMATION FOR A MANY-COMPONENT SYSTEM

In this Appendix, we generalize the elastic treatment for a one-component system found in Gao *et al.* [16] to a generic many-component system in dimension D. We start from the potential energy (see Eq. (55) of Ref. [16]) duly generalized to a many-component system,

$$W[\mathbf{u}] = \frac{1}{2} \sum_{\alpha,\beta} \int d\mathbf{r} \int d\mathbf{r}' \rho_{\alpha\beta}^{(2)}(\mathbf{r}, \mathbf{r}') \phi_{\alpha\beta}(|\mathbf{r} + \mathbf{u}_\alpha(\mathbf{r}) - \mathbf{r}' - \mathbf{u}_\beta(\mathbf{r}')|), \tag{A1}$$

with $\phi_{\alpha\beta}(r)$ the interparticle potentials, $\rho_{\alpha\beta}^{(2)}(\mathbf{r}, \mathbf{r}')$ the two-body densities and $\mathbf{u}_\alpha(\mathbf{r})$ the displacement field of the species α. Below we shall denote with $u_{\alpha;\mu}(\mathbf{r})$ the Cartesian component μ of the $D-$dimensional vector $\mathbf{u}_\alpha(\mathbf{r})$. Following Gao *et al.*, we expand the potential energy in powers of the displacement fields to second order, obtaining

$$W_2[\mathbf{u}] = -\frac{1}{2} \sum_{\alpha,\beta;\mu,\nu} \frac{1}{2} \int d\mathbf{r} \int d\mathbf{r}' [K_{\alpha\beta}(\mathbf{r}, \mathbf{r}')]_{\mu\nu} [u_{\alpha;\mu}(\mathbf{r}) - u_{\beta;\mu}(\mathbf{r}')][u_{\alpha;\nu}(\mathbf{r}) - u_{\beta;\nu}(\mathbf{r}')], \tag{A2}$$

where

$$[K_{\alpha\beta}(\mathbf{r}, \mathbf{r}')]_{\mu\nu} = \rho_{\alpha\beta}^{(2)}(\mathbf{r}, \mathbf{r}') \frac{\partial^2 \phi_{\alpha\beta}(|\mathbf{r} - \mathbf{r}'|)}{\partial r_\mu \partial r'_\nu}. \tag{A3}$$

In a homogeneous isotropic liquid,

$$\rho_{\alpha\beta}^{(2)}(\mathbf{r}, \mathbf{r}') = \rho_\alpha \rho_\beta g_{\alpha\beta}(|\mathbf{r} - \mathbf{r}'|) = \rho_{\alpha\beta}^{(2)}(|\mathbf{r} - \mathbf{r}'|), \tag{A4}$$

and therefore

$$[K_{\alpha\beta}(\mathbf{r} - \mathbf{r}')]_{\mu\nu} = \rho_{\alpha\beta}^{(2)}(|\mathbf{r} - \mathbf{r}'|) \frac{\partial^2 \phi_{\alpha\beta}(|\mathbf{r} - \mathbf{r}'|)}{\partial r_\mu \partial r_\nu'}. \tag{A5}$$

We then use the definition of partial structure factors

$$S_{\alpha\beta}(q) = \delta_{\alpha\beta} + \sqrt{\rho_\alpha \rho_\beta} \int d\mathbf{r}[g_{\alpha\beta}(r) - 1] \exp(i\mathbf{q} \cdot \mathbf{r}), \tag{A6}$$

or, equivalently,

$$S_{\alpha\beta}(q) = \delta_{\alpha\beta} + \sqrt{\rho_\alpha \rho_\beta} \int d\mathbf{r} g_{\alpha\beta}(r) \exp(i\mathbf{q} \cdot \mathbf{r}) - (2\pi)^D \sqrt{\rho_\alpha \rho_\beta} \delta(\mathbf{q}), \tag{A7}$$

to get the Fourier transform of the two-body densities:

$$\rho_{\alpha\beta}^{(2)}(q) = \sqrt{\rho_\alpha \rho_\beta}[S_{\alpha\beta}(q) - \delta_{\alpha\beta} + (2\pi)^D \sqrt{\rho_\alpha \rho_\beta} \delta(\mathbf{q})]. \tag{A8}$$

This yields, for the Fourier transform of $[K_{\alpha\beta}(r)]_{\mu\nu}$,

$$[K_{\alpha\beta}(\mathbf{q})]_{\mu\nu} = \sqrt{\rho_\alpha \rho_\beta} \int \frac{d\mathbf{q}'}{(2\pi)^D}[S_{\alpha\beta}(|\mathbf{q} - \mathbf{q}'|) - \delta_{\alpha\beta} + (2\pi)^D \sqrt{\rho_\alpha \rho_\beta} \delta(\mathbf{q} - \mathbf{q}')] q_\mu' q_\nu' \tilde{\phi}_{\alpha\beta}(q')$$

$$= \sqrt{\rho_\alpha \rho_\beta} \int \frac{d\mathbf{q}'}{(2\pi)^D}[S_{\alpha\beta}(|\mathbf{q} - \mathbf{q}'|) - \delta_{\alpha\beta}] q_\mu' q_\nu' \tilde{\phi}_{\alpha\beta}(q') + \rho_\alpha \rho_\beta q_\mu q_\nu \tilde{\phi}_{\alpha\beta}(q). \tag{A9}$$

To write the equation of motions for the displacement fields, we need

$$X_{\gamma;\lambda}(\mathbf{q}) = \int d\mathbf{r} \frac{\partial W_2[\mathbf{u}]}{\partial u_{\gamma;\lambda}(\mathbf{r})} \exp(i\mathbf{q} \cdot \mathbf{r}). \tag{A10}$$

From Eq. (A2), we get

$$\frac{\partial W_2[\mathbf{u}]}{\partial u_{\gamma;\lambda}(\mathbf{r})} = -\sum_{\beta;\nu} \int d\mathbf{r}' K_{\gamma\beta;\lambda\nu}(|\mathbf{r} - \mathbf{r}'|)[u_{\gamma;\nu}(\mathbf{r}) - u_{\beta;\nu}(\mathbf{r}')], \tag{A11}$$

which, combined with Eq. (A9), yields

$$X_{\gamma;\lambda}(\mathbf{q}) = -\sum_{\beta;\nu} \{[K_{\gamma\beta}]_{\lambda\nu}(\mathbf{q} = 0) u_{\gamma;\nu}(\mathbf{q}) - [K_{\gamma\beta}]_{\lambda\nu}(\mathbf{q}) u_{\beta;\nu}(\mathbf{q})\} \tag{A12}$$

$$= \sum_{\beta;\nu} \left[\left(-\sqrt{\rho_\gamma \rho_\beta} \int \frac{d\mathbf{q}'}{(2\pi)^D}[S_{\gamma\beta}(q') - \delta_{\gamma\beta}] q_\lambda' q_\nu' \tilde{\phi}_{\gamma\beta}(q') - \rho_\gamma \rho_\beta q_\lambda q_\nu \tilde{\phi}_{\gamma\beta}(q)|_{q=0} \right) u_{\gamma;\nu}(\mathbf{q}) \right.$$

$$\left. \times \left(\sqrt{\rho_\gamma \rho_\beta} \int \frac{d\mathbf{q}'}{(2\pi)^D}[S_{\gamma\beta}(|\mathbf{q} - \mathbf{q}'|) - \delta_{\gamma\beta}] q_\lambda' q_\nu' \tilde{\phi}_{\gamma\beta}(q') + \rho_\gamma \rho_\beta q_\lambda q_\nu \tilde{\phi}_{\gamma\beta}(q) \right) u_{\beta;\nu}(\mathbf{q}) \right]. \tag{A13}$$

For the kinetic energy term using Eqs. (27), (52), (53) of Ref. [16], we obtain for a homogeneous Fermion system in dimension D,

$$Y_{\gamma;\lambda}(\mathbf{q}) = \frac{\partial T_2[\mathbf{u}]}{\partial \mathbf{u}_\gamma(\mathbf{q})} = \frac{2}{D} \rho_\gamma t(\rho_\gamma)[2q_\lambda(\mathbf{q} \cdot \mathbf{u}_\gamma(\mathbf{q})) + q^2 u_\gamma(\mathbf{q})] + \frac{\rho_\gamma}{4m_\gamma} \hbar^2 q^2 q_\lambda(\mathbf{q} \cdot \mathbf{u}_\gamma(\mathbf{q})), \tag{A14}$$

with m_γ the mass and $t(\rho_\gamma)$ the interacting kinetic energy per particle of the species γ. The equation of motion for the species γ thus becomes

$$m_\gamma \rho_\gamma \omega^2(\mathbf{q}) \mathbf{u}_\gamma(\mathbf{q}) = \mathbf{Y}_\gamma(\mathbf{q}) + \mathbf{X}_\gamma(\mathbf{q}), \tag{A15}$$

with $\mathbf{Y}_\gamma(\mathbf{q})$ and $\mathbf{X}_\gamma(\mathbf{q})$ vectors with Cartesian components $X_{\gamma;\lambda}(\mathbf{q})$ and $Y_{\gamma;\lambda}(\mathbf{q})$, i.e.,

$$\mathbf{X}_\gamma(\mathbf{q}) = \sum_\beta \left[\left(-\sqrt{\rho_\gamma \rho_\beta} \int \frac{d\mathbf{q}'}{(2\pi)^D}[S_{\gamma\beta}(q') - \delta_{\gamma\beta}] \tilde{\phi}_{\gamma\beta}(q') \mathbf{q}'(\mathbf{q}' \cdot \mathbf{u}_\gamma(\mathbf{q})) - \rho_\gamma \rho_\beta \tilde{\phi}_{\gamma\beta}(q_0) \mathbf{q}_0(\mathbf{q}_0 \cdot \mathbf{u}_\gamma(\mathbf{q}))|_{q_0=0} \right) \right.$$

$$\left. + \left(\sqrt{\rho_\gamma \rho_\beta} \int \frac{d\mathbf{q}'}{(2\pi)^D}[S_{\gamma\beta}(|\mathbf{q} - \mathbf{q}'|) - \delta_{\gamma\beta}] \tilde{\phi}_{\gamma\beta}(q') \mathbf{q}'(\mathbf{q}' \cdot \mathbf{u}_\beta(\mathbf{q})) + \rho_\gamma \rho_\beta \tilde{\phi}_{\gamma\beta}(q) \mathbf{q}(\mathbf{q} \cdot \mathbf{u}_\beta(\mathbf{q})) \right) \right] \tag{A16}$$

and

$$\mathbf{Y}_\gamma(\mathbf{q}) = \frac{\partial T_2[\mathbf{u}]}{\partial \mathbf{u}_\gamma(\mathbf{q})} = \frac{2}{D} \rho_\gamma t(\rho_\gamma)[2\mathbf{q}(\mathbf{q} \cdot \mathbf{u}_\gamma(\mathbf{q})) + q^2 \mathbf{u}_\gamma(\mathbf{q})] + \frac{\rho_\gamma}{4m_\gamma} \hbar^2 q^2 \mathbf{q}(\mathbf{q} \cdot \mathbf{u}_\gamma(\mathbf{q})). \tag{A17}$$

[1] S. De Palo, F. Rapisarda, and G. Senatore, Phys. Rev. Lett. **88**, 206401 (2002).

[2] G. Senatore and S. D. Palo, Contrib. Plasma Phys. **43**, 363 (2003).

[3] J. Shumway and M. J. Gilbert, Phys. Rev. B **85**, 033103 (2012).

[4] R. Maezono, P. López Ríos, T. Ogawa, and R. J. Needs, Phys. Rev. Lett. **110**, 216407 (2013).

[5] R. O. Sharma, L. K. Saini, and B. P. Bahuguna, Phys. Rev. B **94**, 205435 (2016).

[6] F. Tramonto, Stefania De Palo, Saverio Moroni, and Gaetano Senatore, Conference on Frontiers in Two-Dimensional Quantum Systems, 13–17 November 2017, ICTP, Trieste, Italy (unpublished).

[7] J. P. Eisenstein and A. H. MacDonald, Nature (London) **432**, 691 (2004).

[8] E. Tutuc, M. Shayegan, and D. A. Huse, Phys. Rev. Lett. **93**, 036802 (2004).

[9] S. Conti, M. Van der Donck, A. Perali, F. M. Peeters, and D. Neilson, Phys. Rev. B **101**, 220504(R) (2020).

[10] M. Van der Donck, S. Conti, A. Perali, A. R. Hamilton, B. Partoens, F. M. Peeters, and D. Neilson, Phys. Rev. B **102**, 060503(R) (2020).

[11] Z. Wang, D. A. Rhodes, K. Watanabe, T. Taniguchi, J. C. Hone, J. Shan, and K. F. Mak, Nature (London) **574**, 76 (2019).

[12] L. Ma, P. X. Nguyen, Z. Wang, Y. Zeng, K. Watanabe, T. Taniguchi, A. H. MacDonald, K. F. Mak, and J. Shan, arXiv:2104.05066 (2021).

[13] G. Vignale and A. H. MacDonald, Phys. Rev. Lett. **76**, 2786 (1996).

[14] G. W. Burg, N. Prasad, K. Kim, T. Taniguchi, K. Watanabe, A. H. MacDonald, L. F. Register, and E. Tutuc, Phys. Rev. Lett. **120**, 177702 (2018).

[15] G. E. Santoro and G. F. Giuliani, Phys. Rev. B **37**, 937 (1988).

[16] X. Gao, J. Tao, G. Vignale, and I. V. Tokatly, Phys. Rev. B **81**, 195106 (2010).

[17] S. M. Girvin, A. H. MacDonald, and P. M. Platzman, Phys. Rev. B **33**, 2481 (1986).

[18] G. Kalman, V. Valtchinov, and K. I. Golden, Phys. Rev. Lett. **82**, 3124 (1999).

[19] Z. Donkó, G. J. Kalman, P. Hartmann, K. I. Golden, and K. Kutasi, Phys. Rev. Lett. **90**, 226804 (2003).

[20] K. I. Golden, H. Mahassen, G. J. Kalman, G. Senatore, and F. Rapisarda, Phys. Rev. E **71**, 036401 (2005).

[21] K. I. Golden, H. Mahassen, G. Senatore, and F. Rapisarda, Phys. Rev. E **74**, 056405 (2006).

[22] G. Giuliani and G. Vignale, *Quantum Theory of the Electron Liquid* (Cambridge University Press, New York, 2005).

[23] K. I. Golden and G. J. Kalman, J. Phys. A: Math. Gen. **36**, 5865 (2003).

[24] Y. Zeng and A. H. MacDonald, Phys. Rev. B **102**, 085154 (2020).

[25] G. D. Mahan, *Many Particle Physics* (Plenum Press, New York, 1981).

[26] X. Zhu, P. B. Littlewood, M. S. Hybertsen, and T. M. Rice, Phys. Rev. Lett. **74**, 1633 (1995).

[27] P. B. Littlewood and X. Zhu, Phys. Scr. **T68**, 56 (1996).

[28] The third-moment sum rule for a system with two types of particles can be immediately obtained from Eq. (3.206) for the spin-dependent third moments of an electron gas [22]; one changes the Coulomb interaction into pair interactions dependent on the spin indexes, to then be interpreted as type indexes. Note that the third moment here is denoted with $M(q)q^2$, whereas in Ref. [22] it is denoted with $M(q)$.